Published in final edited form as:
Nat Microbiol. 2017 January 13; 2: 16258. doi:10.1038/nmicrobiol.2016.258.

EspL is a bacterial cysteine protease effector that cleaves RHIM proteins to block necroptosis and inflammation

Jaclyn S. Pearson[1,*], **Cristina Giogha**[1,*], **Sabrina Mühlen**[1,∞], **Ueli Nachbur**[2,3], **Chi L. L. Pham**[4], **Ying Zhang**[1], **Joanne M. Hildebrand**[2,3], **Clare V. Oates**[1], **Tania Wong Fok Lung**[1], **Danielle Ingle**[1], **Laura F. Dagley**[2,3], **Aleksandra Bankovacki**[2,3], **Emma J. Petrie**[2,3], **Gunnar N. Schroeder**[5,^], **Valerie F. Crepin**[5], **Gad Frankel**[5], **Seth L. Masters**[2,3], **James Vince**[2,3], **James M. Murphy**[2,3], **Margaret Sunde**[4], **Andrew I. Webb**[2,3], **John Silke**[2,3], **Elizabeth L. Hartland**[1,#]

[1]Department of Microbiology and Immunology, University of Melbourne at the Peter Doherty Institute for Infection and Immunity, Melbourne 3000, Australia

[2]The Walter and Eliza Hall Institute of Medical Research, Parkville, Victoria 3052, Melbourne, Australia

[3]Department of Medical Biology, University of Melbourne, Victoria 3010, Australia

[4]Discipline of Pharmacology, School of Medical Sciences, University of Sydney, New South Wales 2006, Australia

[5]MRC Centre for Molecular Bacteriology and Infection, Department of Life Sciences, Imperial College London, SW7 2AZ, UK

Abstract

Cell death signalling pathways contribute to tissue homeostasis and provide innate protection from infection. Adaptor proteins such as RIPK1, RIPK3, TRIF and ZBP1/DAI that contain receptor-interacting protein (RIP) homotypic interaction motifs (RHIM) play a key role in cell death and inflammatory signalling [1–3]. RHIM-dependent interactions help drive a caspase independent form of cell death termed necroptosis [4,5]. Here we report that the bacterial pathogen enteropathogenic *Escherichia coli* (EPEC) uses the type III secretion system (T3SS) effector EspL to degrade the RHIM containing proteins, RIPK1, RIPK3, TRIF and ZBP1/DAI during infection. This required a previously unrecognised tripartite cysteine protease motif in EspL (Cys^{47}, His^{131}, Asp^{153}) that cleaved within the RHIM of these proteins. Bacterial infection and/or ectopic expression of EspL led to rapid inactivation of RIPK1, RIPK3, TRIF and ZBP1/DAI and inhibition of TNF, LPS or poly(I:C)-induced necroptosis and inflammatory signalling. Furthermore, EPEC infection inhibited TNF-induced phosphorylation and plasma membrane localization of MLKL. *In vivo*, EspL cysteine protease activity contributed to persistent colonization of mice by the EPEC-like

[#]Correspondence: hartland@unimelb.edu.au.
[*]equal contribution
[∞]Current address: Department of Molecular Infection Biology, Helmholtz-Centre for Infection Research, 38124 Braunschweig, Germany
[^]Current address: Centre for Experimental Medicine, Queen's University Belfast, BT9 7BL, UK

Author contributions. J.S.P., C.G., S. M., U. N, C.L.L.P., Y.Z., J.M.H., T.W., D. I., A.B., E. J. P. J.V. and M.S. designed and performed the experiments. S.L.M., J.M., G.N.S., C.V.O., V.F.C. and G.F contributed reagents and expertise. L.F.D. and A.I.W. performed mass spectrometry analyses. J.S.P. C. G, J.S. and E.L.H. designed the experiments and wrote the manuscript.

Europe PMC Funders Author Manuscripts

mouse pathogen *Citrobacter rodentium*. The activity of EspL defines a family of T3SS cysteine protease effectors found in a range of bacteria and reveals a mechanism by which gastrointestinal pathogens directly target RHIM-dependent inflammatory and necroptotic signalling pathways.

Keywords

EPEC; necroptosis; RHIM; cysteine protease

RHIM containing proteins, including RIPK1, RIPK3, TRIF and ZBP1/DAI, play essential roles in the regulation of inflammatory and cell death-signalling pathways [5]. RIPK1 is a key regulator of the NF-κB signalling pathway in response to TNF/TNFR1 stimulation, and may induce apoptosis through formation of a cytosolic complex containing TRADD/FADD and caspase-8 [6]. However, upon inhibition of caspase-8 activity, RIPK1 binds RIPK3 through RHIM-RHIM interactions leading to phosphorylation of RIPK3 and the recruitment and phosphorylation of MLKL by activated RIPK3 [7–11]. Phosphorylated oligomeric MLKL translocates to the plasma membrane, which leads to the caspase independent form of cell death termed necroptosis [12,13]. Necroptosis may also result from TRIF or DAI/ZBP1 interactions with RIPK1 and RIPK3, which are also mediated by RHIM-RHIM interactions [14,15]. In addition, RIPK3 can promote NLRP3 inflammasome activation independently of necroptosis that is thought to be triggered by RHIM-RHIM amyloid formation [16].

Infection of intestinal epithelial cells with the attaching and effacing enteropathogen, EPEC, leads to rapid inhibition of host inflammatory and apoptosis signalling pathways due to the activity of T3SS effectors [17]. While studying the effect of EPEC infection on assembly of the TNFR1 receptor complex, we observed that RIPK1 was rapidly degraded during wild type EPEC infection (E2348/69) but not during infection with the T3SS mutant *(ΔescN)* (Supplementary Figure 1a). By testing derivatives of EPEC lacking the genomic islands *PP4* alone *(ΔPP4)* or *PP4* and *IE6 (ΔPP4/IE6)*, we identified *IE6* and subsequently the gene encoding the effector EspL as essential for T3SS-dependent RIPK1 degradation (Fig. 1a; Supplementary Figure 1b). *espL* is located upstream of the T3SS effector genes, *nleB1* and *nleE*, which encode known inhibitors of apoptosis and NF-κB activation respectively (Fig. 1a) [18–20]. We confirmed that EspL was translocated by the T3SS using the TEM1 β-lactamase reporter [21] and that deletion of *espL* had no impact on actin accretion by EPEC, a measure of adherence and T3SS activity (Supplementary Figure 1c-e).

In mammalian cells, RIPK1 may be removed by K48-linked ubiquitylation and proteosomal degradation or by caspase-mediated cleavage [22–24]. However, neither caspase nor proteasome inhibitors, z-VAD-FMK (z-VAD) and MG132 respectively, prevented EspL-dependent loss of RIPK1 (Fig. 1b). Therefore, we speculated that EspL might mediate direct degradation of RIPK1. Although amino acid sequence analysis failed to uncover any canonical protease motifs, alignment of EspL with homologues identified by BLAST [25] from a range of bacterial pathogens revealed a putative conserved cysteine protease motif with the possible catalytic residues Cys^{47}, His^{131} and Asp^{153} (Fig. 1c, d, 2a; Supplementary Figure 2). Despite lacking primary amino acid sequence similarity with known cysteine proteases, the secondary structure of EspL predicted by Phyre [26] showed N-terminal

Europe PMC Funders Author Manuscripts

similarity to the CA clan of papain-like cysteine proteases, which includes the unrelated T3SS effector YopT from *Yersinia* spp. (Fig. 1c) [27]. Despite this, the broad spectrum cysteine protease inhibitors, antipain and Z-FA-FMK had no or only weak effect on EspL activity (Supplementary Figure 1f). Complementation of EPEC strain *ΔPP4*/E6 or the *ΔespL* mutant with native EspL expressed *in trans* restored RIPK1 degradation. However, alanine substitution of Cys^{47}, His^{131} and Asp^{153} but not Cys^{40} abrogated EspL-induced RIPK1 degradation, confirming the crucial role of these amino acids in EspL activity (Fig. 1d).

To determine the specificity of EspL for RIPK1 degradation, we examined the effect of EPEC infection on human as well as murine RIP kinases by immunoblot. In addition to RIPK1, catalytically active EspL also induced loss of RIPK3, which shares a high degree of similarity with RIPK1 [28] (Fig. 1d, Supplementary Figure 3a). Levels of RIPK2 were unaffected by EspL. Using an antibody generated to residues 385-650 of RIPK1, we detected a ~14 kDa cleavage product following ectopic expression of codon optimised Flag-EspL in HEK293T cells, suggesting that EspL removed the C-terminus of RIPK1 which encompasses the RHIM (Supplementary Figure 3b). To test the ability of EspL to cleave all mammalian RHIM containing proteins directly, we incubated purified recombinant EspL with the purified RHIM-containing regions of RIPK1, RIPK3, TRIF and ZBP1 and observed cleavage by catalytically active EspL for all RHIM proteins (Fig. 2b). Intact mass spectrometry and N-terminal sequencing of the cleavage products from RIPK3 and TRIF identified the cleavage site as QxGxx↓N (P5-P4-P3-P2-P1-P1') (Fig. 2b, c, Supplementary Figure 3c, d). Substitution of V^{448}, Q^{449}, I^{450} and G^{451} with alanine abrogated the ability of EspL to cleave RIPK3 during EPEC infection suggesting that this conserved RHIM sequence was important for substrate recognition by EspL (Supplementary Figure 3e). EspL also possessed the ability to cleave the viral RHIM containing protein M45 from MCMV (Supplementary Figure 3f).

Given the observed cleavage of RIPK1 and RIPK3, we hypothesised that EspL would prevent RIPK1/RIPK3-dependent necroptosis. Mouse dermal fibroblasts (MDF) were used to create stable, doxycycline inducible cell lines expressing EspL or $EspL_{C47S}$. Induction of catalytically active EspL was coincident with loss of RIPK1 and RIPK3 and this effect was reversible upon removal of induction (Supplementary Figure 4a, b). Cells expressing EspL were protected from necroptotic cell death, as measured by PI uptake, when induced by treatment with TNF, QVD or z-VAD (as caspase inhibitors) and the Smac-mimetic IAP antagonist, compound A (Cp.A) as an inhibitor of NF-κB activation [29]. These conditions are known to induce cell death by necroptosis [13]. This protection required EspL activity (Supplementary Figure 4c, 5a, b). EspL expression in MDF cells also prevented MLKL oligomerization and membrane translocation (Supplementary Figure 5c), two hallmarks of necroptosis [13]. During infection, EPEC blocked MLKL phosphorylation, oligomerization and membrane translocation and consequently necroptosis in HT-29 cells in an EspL dependent manner (Fig. 3, Supplementary Figure 6).

Apart from EspL, the T3SS effector NleB1 from EPEC can block TNF induced necroptosis by modifying a conserved arginine in the death domain of RIPK1 with *N*-acetyl glucosamine (GlcNAc) [19]. Consistent with partial redundancy in EspL and NleB1 function,

only EPEC derivatives lacking both *espL* and *nleB1 (ΔPP4/IE6* or *ΔespLnleBE)* were unable to inhibit TNF-induced necroptosis (Fig. 3b; Supplementary Figure 6). In addition, complementation of *ΔPP4/IE6* with either active EspL or NleB but not NleE, restored EPEC-mediated inhibition of necroptosis whereas inactive EspL ($EspL_{C47S}$) or NleB1 (NleB1AAA) [18,19] did not (Fig. 3, Supplementary Figure 6).

Consistent with loss of RIPK1, ectopic expression of EspL, but not inactive EspL, blocked TNF-induced expression of an NF-κB dependent luciferase reporter (Supplementary Figure 7a). In addition, EspL delivered by the T3SS in the EPEC mutant background *ΔPP4/IE6* resulted in reduced IL-8 production by infected HT-29 cells (Supplementary Figure 7b). EspL dependent loss of TRIF following EPEC infection or ectopic expression resulted in impaired interferon-β *(Infβ)* expression and necroptosis induced by the TLR3 and TLR4 ligands, poly(I:C) and LPS, respectively (Fig. 4a, b, Supplementary Figure 7c). Using immortalised bone marrow derived macrophages (iBMDM), we observed that EspL blocked NLRP3/RIPK3-dependent caspase-1 activation induced by treatment with Cp.A/QVD [16], whereas activation of the canonical NLRP3 inflammasome by nigericin was unaffected (Supplementary Figure 7d).

Although EspL possessed the ability to cleave all mammalian RHIM-containing proteins, a time course comparing RIPK1 and RIPK3 cleavage suggested that RIPK1 was the preferred target during EPEC infection (Supplementary Figure 8a). In addition, cleavage likely occurred before amyloid formation as RHIM fibrils were only inefficiently cleaved by EspL compared to the monomeric proteins (Supplementary Figure 8b, c). Amyloid fibrils form the signalling scaffold of the necrosome and arise from RHIM-RHIM interactions between RIPK1 and RIPK3 [4].

The targeted inhibition of necroptosis and RHIM-dependent inflammatory signalling by EspL during EPEC infection suggested that the activity of EspL might aid mucosal immune evasion. Here we assessed the ability of derivatives of the EPEC-like mouse pathogen, *C. rodentium* to colonise wild type C57BL/6 mice. *C. rodentium* is a murine attaching and effacing pathogen that carries all the conserved T3SS effector genes present in EPEC, including *espL*. We confirmed that EspL from *C. rodentium* (CREspL) cleaved RIPK1, whereas inactive $CREspL_{C42S}$ did not (Fig. 4c). In wild type C57BL/6 mice, we observed that an *espL* mutant of *C. rodentium* was attenuated for intestinal colonization in the resolving phase of infection suggesting that EspL promoted bacterial persistence in the gut, similar to previous findings [30] (Supplementary Figure 9). Complementation of the *espL* mutant with *espL* but not $espL_{C47S}$ restored intestinal colonization by *C. rodentium* (Fig. 4d) suggesting that the cysteine protease activity of EspL was critical to its virulence function. Given the semi-redundant activities of EspL and NleB1 that we observed in the inhibition of necroptosis, and the fact that *nleB* mutants of *C. rodentium* also exhibit a colonization defect [18,19], further work should examine the relative contribution of each effector in vivo using an *espL/nleB* double mutant of *C. rodentium* complemented with active and inactive forms of NleB and EspL.

Here we have defined EspL from EPEC as the prototypic member of a family of T3SS cysteine protease effectors and identified the targets of EspL as host RHIM-containing

proteins. EspL inactivated inflammatory, inflammasome and necroptotic signalling by cleaving within the RHIM, thereby disrupting a range of host mucosal defence pathways. EspL adds to the arsenal of bacterial T3SS effectors that subvert host cell signalling and the presence of, as yet uncharacterised, EspL homologues in a broad range of bacterial pathogens suggests that this family of cysteine protease effectors constitutes a widespread virulence mechanism.

Methods

Bacterial strains, plasmids, cell lines and growth conditions

The bacterial strains, plasmids and oligonucleotide primers used in this study are listed in Table S1. Bacteria were grown at 37 °C in Luria-Bertani (LB) medium, Dulbecco's Modified Eagle's medium (DMEM) with GlutaMAX (Gibco, NY), or Roswell Park Memorial Institute medium (RPMI) with GlutaMAX (Gibco) where indicated and supplemented with ampicillin (100 μg/mL), kanamycin (100 μg/mL), nalidixic acid (50 μg/mL) or chloramphenicol (25 μg/mL) where necessary.

Mouse dermal fibroblasts (MDFs) were isolated from the dermis of adult mice and immortalised with SV40 large T antigen [31]. Bone marrow derived macrophages from C57BL/6 mice were immortalized to generate a macrophage cell line (iBMDM) with CreJ2 virus as described previously [32]. All other cell lines were sourced from and authenticated by either the ATCC Global Bioresource Centre, or the ECACC via Sigma-Aldrich. HeLa cells, HEK293T cells, Caco-2 cells, iBMDMs, MDFs and MEFs were grown in DMEM GlutaMax (Gibco) supplemented with 10% FCS (Sigma) at 37 °C with 5% CO_2. HT-29 cells were grown in Roswell Park Memorial Institute medium (RPMI) GlutaMAX (Gibco) with 10% FCS (Sigma) at 37 °C with 5% CO_2.

Construction of EspL expression vectors

For expression in bacteria, the *espL* gene was amplified from EPEC E2348/69 genomic DNA by PCR using the primer pair $EspL_F$/$EspL_R$ for cloning into pTrc99A. PCR amplification consisted of an initial denaturation step at 95 °C for 10 min, followed by 30 cycles of 94 °C for 44 sec, 55 °C for 45 sec and 70 °C for 2 min followed by a final elongation step of 70°C for 10 min. The PCR product was digested with KpnI and EcoRI and ligated into pTrc99A to produce pEspL.

For expression in mammalian cells, the gene encoding EspL from either EPEC E2348/69 or *C. rodentium* ICC169 was codon-optimised (DNA2.0), amplified using the primer pair EspLCOF/EspLCOR or EspLCRCOF/EspLCRCOR and ligated into KpnI/BamHI digested p3XFlag-*Myc*-CMV-24 to generate N-terminal 3xFlag fusions of EspL (pFlag-EspL or pFlag-CREspL). For construction of the lentiviral plasmid to generate stable inducible cell lines, codon optimised Flag-EspL was amplified from pFlag-EspL and ligated into pF TRE3G PGK puro [10,29] using BamHI/XbaI.

Genes encoding residues 2-549 of EPEC E2348/68 EspL and $EspL_{C47S}$ were amplified by PCR using pEspL and $pEspL_{C47S}$ as template DNA respectively, using the primer pair $EspL_{GEXF}$/$EspL_{GEXR}$. PCR products were digested with BamHI and NotI and ligated into

the vector pGEX-2T-TEV, as previously described [33] to enable bacterial expression with an in-frame N-terminal GST fusion. Insert sequences were verified by Sanger sequencing (Micromon, Monash University, Australia).

Site-directed mutagenesis

Site-directed mutants were generated using the Stratagene QuikChange II Site-Directed Mutagenesis Kit according to manufacturer's protocol. pEspL$_{C40s}$, pEspL$_{C47S}$, pEspL$_{H131A}$, pEspL$_{D153A}$ were generated using pEspL as template DNA and primer pairs EspL$_{(C40S)F}$/EspL$_{(C40S)R}$, EspL$_{(C47S)F}$/EspL$_{(C47S)R}$, EspL$_{(H131A)F}$/EspL$_{(H131A)R}$ and EspL$_{(D153A)F}$/EspL$_{(D153A)R}$ respectively. pFlag-EspL$_{C40s}$, pFlag-EspL$_{C47S}$, pFlag-EspL$_{H131A}$, pFlag-EspL$_{D153A}$ were generated using pFlag-EspL as template DNA and primer pairs EspL$_{(C40s)COF}$/EspLtemplate DNA and primer pairs EspL$_{(C40s)COR}$, EspL$_{(C47S)COF}$/EspL$_{(C47S)COR}$, EspL$_{(H131A)COF}$/EspL$_{(H131A)COR}$ and EspL$_{(D153A)COF}$/EspL$_{(D153A)COR}$ respectively. pF TREG-Flag-EspL$_{C47S}$ was generated using pF TREG-Flag-EspL as template DNA and primer pair EspL$_{(C47S)COF}$/EspL$_{(C47S)COR}$. pFlag-CREspL$_{C42S}$ was generated using pFlag-CREspL as template DNA and primer pair EspL$_{C42S(CO)F}$/EspL$_{C42S(CO)R}$. pGEX-EspL$_{C47S}$ was generated by PCR-amplification of a cDNA encoding EPEC E2348/69 EspL$_{C47S}$ (pTrc-EspL$_{C47S}$) using primers EspL$_{GEXF}$/EspL$_{GEXR}$ bearing restriction sites (5' BamHI, 3' NotI), followed by restriction digest and ligation into the vector, pGEX-2T-TEV (pGEX-EspL$_{C47S}$). pGFP-mRIPK3$_{AAAA}$ was generated using pGFP-mRIPK3 as template DNA and primer pair mRIPK3$_{AAAA-F}$/mRIPK3$_{AAAA-R}$.

Purification of GST-EspL

600 mL Super broth cultures containing 100 μg/mL ampicillin were inoculated with *E. coli* BL21 Codon Plus transformed with GST-EspL or GST-EspL$_{C47S}$ expression constructs and cultured at 37 °C with shaking to OD$_{600}$ of 0.6-0.8. Cultures were then cooled to 18 °C, protein expression induced by addition of 1 mM IPTG with continued shaking and incubation at 18 °C overnight. Cell pellets were resuspended in lysis buffer (200 mM NaCl, 20 mM HEPES pH 7.5, 5% w/v glycerol, 0.5 mM TCEP), before lysis by sonication, elimination of debris by centrifugation at 45000 g, 0.45 μm filtration of the lysate and incubation with glutathione agarose (UBP Bio) at 4 °C with agitation for 1-2 h. Beads were collected and washed with lysis buffer before incubation with 200 μg TEV protease at 20 °C for 2 h on rollers. Supernatant containing cleaved EspL or EspL$_{C47S}$ was concentrated by centrifugal ultrafiltration and loaded on to Superdex S200 gel filtration column pre-equilibrated with gel filtration buffer (200 mM NaCl, 20 mM HEPES pH 7.5, 5% v/v glycerol). Fractions containing purified EspL or EspL$_{C47S}$, as assessed by SDS-PAGE, were pooled, concentrated by centrifugal ultrafiltration to 5 mg/mL, aliquoted, snap frozen in liquid nitrogen and stored at -80 °C until required.

RHIM domain protein constructs, expression and purification

Synthetic genes encoding RHIM-containing regions of human RIPK1 (Q13546; residues 497-583), human RIPK3 (Q9Y572; residues 387-518), human DAI/ZBP1 (Q9H171; residues 170-429), human TRIF (Q8IUC6; residues 601-712) with flanking BamHI and EcoRI restriction sites were purchased from Genscript, digested with these restriction enzymes, purified by agarose gel electrophoresis and ligated individually into the pHUE

vector cut with the same two restriction enzymes [34]. All expressed fusion proteins therefore consist of His6-ubiquitin-RHIM region. Successful cloning was confirmed by sequencing at AGRF (Westmead Institute) Sydney. Proteins were expressed in BL21(DE3) grown at 37 °C to an OD_{600} of 0.6-0.8, and induced with 0.5 mM IPTG for 3 h. Cell pellets were lysed in 6M GuHCl, 100 mM NaH_2PO_4, 20 mM Tris.Cl, 5 mM β mercaptoethanol, pH 8.0, and soluble material further purified on Ni-NTA agarose under denaturing conditions, with exchange into 8 M urea, 100 mM NaH_2PO_4, 20 mM Tris, 5 mM β mercaptoethanol at pH 6.0 for washing and pH 4.0 for elution from the Ni-NTA agarose.

Generation of stable inducible cell lines in mouse dermal fibroblasts (MDF) and immortalized bone marrow derived macrophages (iBMDM)

HEK293T cells were seeded at 2 x 10^5 cells per 10 cm culture dishes and 24 h later were co-transfected with 10 μg of either pF TRE3G-Flag-EspL or pF TRE3G-Flag-$EspL_{C47S}$ along with the helper plasmids pMDL-RRE, pRSV-REV and pVSV-g (5, 2.5 and 3 μg, respectively) using Effectine Transfection Reagent (QIAGEN) for a further 24 h. Culture media was then changed and the cells were incubated for a further 48 h for virus production. Polybrene (5 μg/mL) (Sigma) was added to the cell culture dishes and the virus-containing supernatant was collected and passed through a 0.45 μM filter. Virus-containing supernatant was added to either MDF monolayers or iBMDM monolayers and incubated at 37 °C with 5% CO_2 for 24 h. Infected cells were selected for using increasing concentrations of up to 5 μg/mL of puromycin (Sigma) for at least one week. Expression of Flag-EspL or Flag-$EspL_{C47S}$ in either MDFs or iBMDMs was tested by adding 20 ng/mL doxycycline at varying time points followed by immunoblot using anti-Flag antibodies.

Construction of *Citrobacter rodentium espL* mutant

A 325 bp upstream region of *espL* was amplified using primer pair Up-EspL-Fw/BamHI-Up-EspL-Rv, and a 500 bp downstream region of *espL* was amplified using primer pair BamHI-Down-EspL-Fw/Down-EspL-Rv. Both fragments were then digested with BamHI, ligated together, and cloned into pGEMT. The non-polar *aphT* cassette [35] was then inserted into the BamHI site between the two fragments and the orientation of the *aphT* cassette ascertained by PCR. This construct was then amplified using the primer pair Up-EspL-Fw/Down-EspL-Rv. The PCR products were electroporated into ICC169 containing pKD46 encoding lambda red recombinase [36]. Transformants were selected on kanamycin agar plates and *espL* deletion confirmed by PCR (Check-EspL-UP-Fw /Down-EspL-Rv) and DNA sequencing.

cis complementation of the *Citrobacter rodentium espL* mutant

The *Citrobacter rodentium espL* mutant was *cis* complemented with either WT *espL* or *$espL_{C42S}$* using the transgene insertion method previously described [37]. Briefly, the *espL* gene with its native promoter was amplified from *C. rodentium* ICC169 genomic DNA template by PCR using primers $EspL_{CRF1}$/$EspL_{CRR1}$, and then ligated into the XmaI/XhoI restriction sites of the pGRG36 vector. The pGRG36-EspLC42S construct was generated by site-directed mutagenesis. The pGRG36-EspL construct was used as template DNA and amplified by PCR using primers $EspL_{C42SF}$/$EspL_{C42SR}$. The resulting plasmid was digested with DpnI at 37 °C overnight before transformation into the appropriate *E. coli* strain.

The pGRG36-EspL and pGRG36-EspL$_{C42S}$ constructs were confirmed by PCR using primers Tn7$_F$/Tn7$_R$, then electroporated into electrocompetent *C. rodentium espL* mutant cells and selected for using 100 ug/mL ampicillin and incubated at 30 °C overnight. Transformants were streaked out once, then grown overnight in LB without antibiotics at 30 °C. Dilutions were prepared and plated on LB and grown overnight at 42 °C. Transposition of the Tn7:*espL*/*espL*$_{C42S}$ into the *attTn7* insertion site in the *C. rodentium espL* mutant chromosome was confirmed by the absence of the ampicillin resistance marker and PCR using primers CRseqF/CRseqR.

Construction of EPEC single and triple deletion mutants

To construct the EPEC E2348/69 *espL* deletion mutant strain, 342-bp and 331-bp fragments were amplified from 5' and 3' flanking sites of *espL* using oligonucleotides EspL$_{5'F}$/ EspL$_{5'R}$ and EspL$_{3'F}$/ EspL$_{3'R}$. The plasmid pKD4 was used as template DNA to amplify the kanamycin cassette using oligonucleotides pKD3-4F and pKD3-4R. Overlapping PCR was used to assemble the espL flanking regions with the kanamycin cassette construct using oligonucleotides EspL$_{5'F}$ and EspL$_{3'R}$. Lambda red mediated recombination [36] was used to replace the wild type allele with the kanamycin resistance cassette. The cassette was electroporated into wild-type EPEC E2348/69 and positive clones were selected for on LB agar with 25 μg/mL kanamycin. To construct the EPEC E2348/69 *espLnleBE* deletion mutant, a 368-bp fragment was amplified from 5' flanking site of *nleB* using oligonucleotides NleB$_{5'F}$/ NleB$_{5'R}$ and 550-bp fragment was amplified from 3' flanking site of *nleE* using oligonucleotides NleE$_{3'F}$/ NleE$_{3'R}$. The plasmid pKD3 was used as template DNA to amplify the chloramphenicol cassette using oligonucleotides pKD3-4$_F$ and pKD3-4$_R$. Overlapping PCR was used to assemble the *nleB* and *nleE* flanking regions with the chloramphenicol cassette construct using oligonucleotides NleB5T and NleE3¾. Lambda red mediated recombination [36] was used to replace the wild type allele with the chloramphenicol resistance cassette. The cassette was electroporated into EPEC E2348/69 *espL* mutant cells and positive clones were selected for on LB agar with 5 μg/mL chloramphenicol. Deletions were confirmed by PCR with a combination of primers from outside and inside the altered region. Attachment and pedestal formation by parental and mutant strains were confirmed using fluorescence actin staining.

EPEC infection

Cell lines of HeLa, Caco-2, MDF and HT-29 cells are maintained in our laboratory and regularly tested for mycoplasma contamination. Two days prior to infection HeLa, Caco-2, MDF or HT-29 cell monolayers were seeded into 24 well tissue culture trays. One day prior to infection derivatives of EPEC were inoculated into LB broth and grown with shaking at 37 °C overnight. On the day of infection, overnight cultures of EPEC were sub-cultured 1:75 in DMEM GlutaMAX (Gibco) or RPMI GlutaMAX (Gibco) and grown statically for 3 h at 37 °C with 5% CO_2. Where necessary, cells were induced with 1 mM isopropyl-B-D-thiogalactopyranoside IPTG (Sigma) 30 min prior to infection. Cells were washed twice with PBS and infected with EPEC grown to an OD_{600nm} of 0.03 for 1-3 h (depending on the experiment). When required, the inhibitors MG132 (Sigma) (10 μM), antipain (Sigma) (10, 20 or 40 μg/mL), z–VAD-FMK (Abcam) (25 μM), or z-FA-FMK (Abcam) (10, 20 or 40 μM) were added to the cells 1 hr prior to infection and kept on for the duration of the infection.

Transfection

All transfections were performed in HEK293T cells using Fugene® 6 (Promega) transfection reagent. Cells were seeded into 24 well tissue culture trays and transfected 24 h later with 1μg DNA for a period of ~18 h.

Fluorescent actin stain

HeLa cells were seeded on coverslips and infected as previously described. After infection, cells were washed with PBS, fixed in 4 %PFA in PBS for 30 min and permeabilised in 1% Triton X-100 for another 30 min. Cells were then washed twice with PBS and stained with 4',6-diamidino-2-phenylindole (DAPI, Invitrogen) at 0.5 mg/mL and Phalloidin-Tetramethylrhodamine B isothiocyanate (Sigma) in 3% BSA/PBS for 30 min. Coverslips were mounted onto microscope slides with Prolong Gold anti-fade reagent (Invitrogen). Images were acquired using a Zeiss confocal laser scanning microscope with a 1003/EC Epiplan-Apochromat oil immersion objective.

Immunoblot analysis

For immunoblot analysis following EPEC infection, transfection or induction of stable cell lines, cells were collected and lysed in cold lysis buffer (1% Triton X-100, 50 mM Tris-HCl, pH 7.4, 1 mM EDTA, 150 mM NaCl) with Complete Protease Inhibitor (Roche), 2 mM Na_3VO_4, 10 mM NaF, 1 mM PMSF and incubated on ice for 10 min to complete lysis. Samples were then pelleted at 4 °C by centrifugation and the supernatants added to 4×Bolt® LDS Sample Buffer (Thermo Fisher), heated to 70 °C for 10 min and resolved on Bolt® 4-12% Bis-Tris Plus Gels (Thermo Fisher) by PAGE. Proteins were transferred to nitrocellulose membranes using an iBlot2 Gel Transfer Device (Thermo Fisher) and probed with one of the following primary antibodies: mouse monoclonal anti-RIPK1 (38/RIP) (BD Transduction Laboratories), mouse monoclonal anti-RIPK2/RICK (25/RIG-G) (BD Transduction Laboratories), rabbit polyclonal anti-RIPK3 (Abcam) (for HT-29 cells), rabbit polyclonal anti-RIPK3 (ProSci) (for MDF cells) or rabbit polyclonal anti-TRIF (Cell Signaling), mouse monoclonal anti-Flag M2-HRP (Sigma), mouse monoclonal anti-GFP (7.1 and 13.1) (Roche), mouse monoclonal anti-β-actin (AC-15) (Sigma), mouse monoclonal anti-TRADD (7G8) (Cell Signaling), rabbit polyclonal anti-TRAF2 (Cell Signaling), monoclonal rat anti-mouse MLKL (WEHI-3H1) (WEHI, made in-house), mouse monoclonal anti-TEM1 β-lactamase (8A5.A10) (QED Bioscience) diluted in TBS with 5% BSA (Sigma) and 0.1% Tween (Sigma). Proteins were detected using anti-rabbit or anti-mouse IgG secondary antibodies conjugated to horseradish peroxidase (PerkinElmer) diluted in TBS with 5% BSA (Roche) and 0.1% Tween (Sigma) and developed with enhanced chemiluminescence (ECL) western blotting reagent (Amersham). Images were visualised using an MFChemiBis imaging station (DNR, Israel). At least three biological replicates were performed for all experiments.

Cell viability assays (MTT and propidium iodide staining)

For analysis of cell viability using MTT assays, immortalised mouse bone marrow-derived macrophages (iBMDM) stably expressing either EspL or EspLC47S were seeded into 24 well tissue culture plates (Corning) for 18-24 h before being left untreated or treated with

20 ng/mL of LPS (*E. coli* 0111:B4) (Sigma) or 50 μg/mL Poly I:C (for iBMDMs) (Sigma) or 10 μg/mL high molecular weight Poly I:C (InvivoGen, CA, USA) and 10 μM z-VAD-FMK (Abcam) for a further 18 h. The cells were washed once with PBS and replaced with DMEM containing 0.1 μg/mL 3-(4,5-Dimethylthiazol-2-yl)-2,5- diphenyltetrazolium bromide (MTT) (Sigma) for 1 h, after which the medium was removed and 100 μL of dimethyl-sulfoxide (DMSO; Sigma) was added to each well. After thorough mixing on an orbital shaker for 1 min, the absorbance at 540 nm for each well was obtained using a CLARIOstar microplate reader (BMG Labtech, Germany). Results were obtained from at least 3 independent experiments.

For analysis of cell viability by propidium iodide (PI) staining of HT-29 monolayers, cells were seeded into 24 well tissue culture plates with sterile glass coverslips and 48 h later were infected with EPEC derivatives as previously mentioned for 2.5 h followed by 4 h incubation in media supplemented with 50 μg/mL gentamicin and 20 ng/mL TNF (Calbiochem), 500 nM compound A (Cp. A, Tetralogic), 25 μM z-VAD-FMK (Abcam). PI (50 μg/mL) (Sigma) was added for the final 15 min of treatment. Cells were then fixed in 3.7% (wt/vol) formaldehyde (Sigma) in PBS for 10 min and permeabilised with 0.2% Triton (Sigma) for 4 min. 4', 6-diamidino-2-phenylindole (DAPI; Invitrogen) was applied at 0.5 μg/mL in PBS for 10 min. Cells were washed with PBS three times and coverslips were mounted onto microscope slides with Prolong Gold anti-fade reagent (Invitrogen). Images were acquired using a Zeiss confocal laser-scanning microscope with a 100x/EC Epiplan-Apochromat oil immersion objective. Duplicate coverslips were blinded for counting of PI positive cells, and results were obtained from at least 3 independent experiments.

For analysis of cell viability by PI staining and confocal microscopy in MDF cells, EspL and $EspL_{C47S}$ expressing lines were induced with 20 ng/mL doxycycline for 2 h followed by 4 h incubation in media supplemented with 20 ng/mL TNF (Calbiochem), 500 nM Cp. A (Tetralogic), 25 μM z-VAD-FMK (Abcam). PI, DAPI staining and confocal microscopy were carried out as described above. Duplicate coverslips were blinded for counting of PI positive cells, and results were obtained from at least 3 independent experiments.

For analysis of cell viability by PI staining and flow cytometry, MDF-EspL and MDF-$EspL_{C47S}$, cell lines were induced with 10 ng/mL doxycycline for 1 h followed by 24 h incubation in media supplemented with 100 ng/mL hTNF-Fc produced in house (WEHI), 500 nM Cp. A (Tetralogic), 50 μM QVD-OPH (Abcam). Cell death was assessed with PI staining (1 ug/mL) and quantified using a BD FACSCalibur flow cytometer. Data was analysed using the WEASEL Flow Cytometry Software.

Monitoring MLKL complex formation using BN-PAGE

For MDF cells, 5 x 10^5 cells (wild type, stably expressing inducible Flag-EspL or Flag-$EspL_{C47S}$) were used to seed each well of a 6 well tissue culture plate and allowed to attach overnight. Cells were stimulated with 0.5 μg/mL doxycycline for 2 h to induce Flag-EspL expression prior to the addition of 100 ng/mL hTNF-Fc produced in house (WEHI), 500 nM Cp. A (Tetralogic), 25 μM z-VAD-FMK (Abcam) for a further 4 h to induce necroptosis. For HT29 cells, 5 x 10^5 cells were plated in each well of a six well plate and allowed to attach for 48 h. Cells were infected with derivatives of EPEC

E2348/69 for 2.5 h followed by stimulation with 20 ng/mL TNF (Calbiochem), 500 nM Cp. A (Tetralogic), 25 μM z-VAD-FMK (Abcam) for a further 5 h to induce necroptosis. Cells were harvested by scraping and permeabilised in MELB buffer (20 mM HEPES (pH 7.5), 100 mM KCl, 2.5 mM MgCl2, 100 mM sucrose, 0.025% digitonin (BIOSYNTH, Staad, Switzerland) 2 μM N-ethyl maleimide, Complete Protease Inhibitor (Roche) and PhosSTOP phosphatase inhibitor cocktail (Roche)). Cytosolic and crude membrane fractions were separated by centrifugation and the crude membrane fraction further solubilized in MELB buffer containing 1% digitonin and clarified by centrifugation. Digitonin was added to the cytosolic fraction (final 1% w/v) and fractions were resolved on a 4-16% Bis-Tris Native PAGE gels (Thermo Fisher), transferred to PVDF and probed for rabbit anti-human phospho-MLKL (Abcam), monoclonal rat anti-mouse MLKL (WEHI-3H1) (WEHI, made in house), rabbit polyclonal anti-VDAC1 (Millipore) and rabbit polyclonal anti-GAPDH (Cell Signaling).

Inflammasome activation

iBMDMs (WT, EspL or $EspL_{C47S}$) were seeded in 12 well tissue culture treated plates and treated with 50 ng/mL ultra-pure LPS (Invivogen) for 2 h then 1 μg/mL doxycycline (Sigma) added for an additional 2 h. Cells were subsequently stimulated with 1 μM Cp.A (Tetralogic pharmaceuticals) and/or 15 μM QVD-Oph (RnD Systems) for 6 h or 10 μM Nigericin (Sigma) for 1 h. Cell supernatants and lysates were analysed by western blot. Primary antibodies used were mouse monoclonal anti-Flag M2-HRP (Sigma), mouse monoclonal caspase-1 (casper-1) (Adipogen), mouse monoclonal anti-RIPK1 (38/RIP) (BD Transduction), rabbit polyclonal RIPK3 (Axxora; PSC-2283-C100) and mouse monoclonal anti-β-actin (AC-15) (Sigma). All antibody dilutions were performed in 5% skim milk/0.1% PBS Tween.

IL-8 secretion assay

For analysis of IL-8 secretion, HT-29 cell monolayers were infected for 3 h before being incubated for 8-12 h in media supplemented with 50 μg/mL gentamicin with or without 20 ng/mL TNF (Calbiochem, EMD4Biosciences, USA). Following this, the HT-29 cell supernatant was collected and either used immediately or stored at -20 °C for subsequent analysis of IL-8 secretion. IL-8 secretion was measured using the Human IL-8 ELISA MAX Deluxe Set (Biolegend, CA, USA) according to the manufacturer's instructions.

qRT-PCR

Samples for qRT-PCR experiments were DNAse treated using Ambion TURBO DNA-free kit and cDNA synthesis was completed using the iScript™ cDNA synthesis kit (Bio-Rad). qRT-PCR was performed using SsoAdvanced™ Universal $SYBR_{®}$ Green Supermix (Bio-Rad) according to manufacturer's instructions and gene specific primers used are listed in Table S1. Samples were loaded onto MicroAmp® Optical 384-well reaction plates (Life technologies) in duplicate and run on the ABI Quant Studio 7 according to manufacturer's instructions. Melting curve analysis was used to ensure there were no primer dimers. Negative controls included both a no-reverse transcriptase control and a no cDNA control. Data were analysed by the threshold cycle method (ΔΔCt method) [38] and normalised to *18S* abundance. All data are represented as fold induction relative to gene expression

in uninduced, unstimulated cells or uninfected, unstimulated cells. All experiments were carried out in triplicate.

Beta-lactamase translocation assay

HeLa cells were seeded in black 96 well trays with transparent well bottom (Greiner Bio-One) for 16 to 24 h prior to infection. On the day of infection, EPEC strains with derivatives of pCX340 were cultured as previously described. 2.5 mM Probenecid (Sigma) and 1 mM IPTG (Sigma) were added to bacterial cultures for the last 45 min before infection. HeLa cells were loaded with CCF2/AM substrate following manufacturer's instructions (Invitrogen) and incubated at room temperature in the dark for one hour. 15 minutes before infection, cells were transferred back to 37 °C 5% CO_2. Infection was carried out using 50 µl of bacterial culture with an OD_{600} of 0.1 for 60 min at 37 °C in 5% CO_2. Translocation was measured as a ratio of $Emission_{450nm}$:$Emission_{520nm}$ using a CLARIOstar Omega microplate reader (BMGLabtech) using triplicate wells for each strain.

Dual-luciferase reporter assay

For the NF-κB dual-luciferase assay, HeLa cells were seeded into 24-well trays (Corning) and co-transfected with derivatives of p3xFlag-*Myc*-CMV-24 (0.4 µg), 0.05 µg of pRL-TK (Promega, Madison WI, USA) and 0.2 µg of pNF-κB-Luc (Clontech, Palo Alto CA, USA). Approximately 24 h post-transfection, cells were left untreated or stimulated with 20 ng/mL TNF□(Calbiochem, La Jolla, CA) for 6 h. Firefly and Renilla luciferase levels were measured using the Dual-luciferase reporter assay system (Promega) in a CLARIOstar Omega microplate reader (BMGLabtech, Germany). The expression of firefly luciferase was normalised for Renilla luciferase measurements and Luciferase activity was expressed relative to unstimulated p3xFlag-*Myc*-CMV-24-transfected cells.

In vitro cleavage assays

Purified proteins were diluted out of urea-containing buffer and incubated in 100 µl of reaction buffer (25 mM NaH_2PO_4, 150 mM NaCl, 0.5 mM DTT, pH 7.4) at a concentration of 20 µM (RHIM proteins) or 0.9 µM (EspL/$EspL_{C47S}$) for 1 hour at 37 °C. Sample buffer was then added to incubated proteins, before the samples were boiled and subjected to SDS-PAGE on Nu-PAGE 4-12% Bis-Tris polyacrylamide gels. The gels were stained with Coomassie Blue Stain and imaged with a GelMax imager (UVP, Analytik Jena, USA).

To compare the cleavage of RHIM-containing protein in monomeric and fibrillar forms, 10 µg EspL was added to 200 µL of 20 µM of His-Ub-RIPK3 in 25 mM NaH_2PO_4, 150 mM NaCl, 0.5 mM DTT, pH 7.4 immediately following dilution of His-Ub-RIPK3 from 8M urea-containing buffer or after incubation of the diluted His-Ub-RIPK3 for 225 min at 37 °C to allow fibril formation. Samples were subsequently incubated with EspL at 37 °C for 1 h. For both 'monomer' and 'fibril' samples, 100 µL was pelleted at 16,000***g*** for 10 min. The supernatant was collected as the soluble fraction and the pellet was resuspended with 100 µL of 8M urea, pH 4.0. Samples were subjected to SDS-PAGE and stained with Coomassie Blue Stain for visualisation and imaging as above.

Thioflavin-T (ThT) assays

Thioflavin-T (ThT) assays were used to monitor fibril formation. 20μM of recombinant RHIM containing His-Ub-RIPK3 was incubated in buffer (25 mM NaH_2PO_4, 150 mM NaCl, 0.5 mM DTT, pH 7.4, 40 μM ThT) in a Costar 96-well plate (Corning) at 37 °C for 3.75 hours inside a POLARstar Omega microplate reader (BMGLabtech). Samples were excited at 440 nm and ThT fluorescence emission was measured at 480 nm every 60 seconds. Fibril formation was evident after 225 min. To test the cleavage of RHIM fibrils by EspL, 500 μl of 20 μM of His-Ub-RIPK3 was dialysed against 1 L of dialysis buffer (25 mM NaH_2PO_4, 150 mM NaCl, 0.5 mM DTT, pH 7.4) for 24 h at room temperature. 100 μl of 'fibril' sample was then incubated with 0.9 μM purified EspL, vortexed briefly and incubated at 37 °C for either 1 or 2 h. For both 'monomer' and 'fibril' samples, 100 μl was pelleted at 16,000 g for 10 min. The supernatant was collected as the soluble fraction and the pellet was resuspended with 100 μl of 8M urea, pH 4.0. Samples were subjected to SDS-PAGE and stained with Coomassie Blue Stain for visualisation and imaging as previously mentioned.

Reverse-phase HPLC

200-1000 μL of purified RHIM proteins at a concentration of 20 μM were incubated with or without 0.9 μM of purified EspL for 1 hour at 37 °C. Proteins were then analysed by RP-HPLC using a C_8 VYDAC column running in MilliQ water containing 0.1% TFA, 10% methanol and eluted with an increasing gradient of acetonitrile. Peaks were collected and lyophilized for further analysis by N-terminal sequencing or LC-MS/MS.

N-terminal sequencing

N-terminal sequencing was performed by the Australian Proteome Analysis Facility (APAF) at Macquarie University, New South Wales, Australia.

Characterisation of His_6-Ub-RIPK3 and His_6-Ub-TRIF cleavage products by intact mass spectrometry analysis

Characterisation of RIPK3 and TRIF cleavage products by intact mass spectrometry were performed on samples prepared by *in vitro* cleavage assay and purified by RP-HPLC as described above.

Time-of-flight tandem mass spectrometry—Mass measurements of the intact protein ions and ETD and CID MS/MS were performed on the high resolution, high mass accuracy quadrupole time-of-flight (qTOF) mass spectrometer (maXis II UHR qTOF, Bruker Daltonics, Bremen, Germany) equipped with an electrospray ion (ESI) source for the direct-infusion method. For the direct-infusion experiments a flow rate of 180 μL/min was provided by a syringe pump (KdScientific, Holliston, MA, USA) using a 25 μL syringe (SGE Analytical Sciences, VIC, AUS). The following settings were applied: capillary voltage of 4.5 kV, end plate offset of 500 V, mass range of *m/z* 450 to 2500, dry gas of 4.0 L/min, and drying temperature of 220 °C. Nano-ESI infusion was performed using HPLC fractions which were reconstituted in 20 μl of water and diluted 1:10 with 50% acetonitrile: 50% water containing 1% formic acid.

Data analysis—The MS and MS/MS spectra were analyzed using a dedicated top-down data analysis procedure. Briefly, precursor and product ion mass spectra were summed over the infusion time in each MS and MS/MS experiment with Data Analysis software version 4.3 (Bruker Daltonics). Automatic data analysis was performed by deisotoping keeping only the monoisotopic masses followed by charge state deconvolution (SNAP 2 algorithm). The obtained mass list of product ions was matched on the predicted cleaved mRIPK3 sequence to determine the product ion identity and the sequence coverage using the observed mass of the precursor ion.

Necroptosis experiments

The human epithelial cell line, HT-29, as well as mouse dermal fibroblasts (MDF) and immortalised bone marrow derived macrophages (iBMDMs) either infected with derivatives of EPEC E2348/69 or engineered to express EspL derivatives were used to examine the effect of EspL on necroptosis. Necroptosis was induced by treatment with 1) 20 ng/mL TNF, 500 nM Cp.A and 25 μM z–VAD-FMK or 50 μM QVD-OPH or 2) 20 ng/mL of LPS *(E. coli* 0111:B4) and 10 μM z–VAD-FMK or 3) 50 μg/mL Poly I:C (for iBMDMs) or 10 μg/mL high molecular weight Poly I:C (for HT-29) and 10 μM z–VAD-FMK. Cell viability was assessed by reduction of 3-(4,5-Dimethylthiazol-2-yl)-2,5- diphenyltetrazolium bromide (MTT) or by propidium iodide (PI) uptake. MLKL complex formation and membrane translocation were examined by Blue native PAGE of cell membrane and cytosolic fractions and immunoblotting using antibodies to MLKL and phospho-MLKL.

Protein sequence alignment and phylogenetic tree

RHIM domain alignment for human and mouse RIPK1, RIPK3, TRIF and DAI was performed by Clustal Omega and ESPript3[39]. Accession numbers (same order as displayed in Fig. 2c) NP_003795, NP_033094, NP_006862, NP_064339, NP_891549, NP_778154, NP_110403, NP_067369, NP_001153889, NP_001132991. For comparison of the cysteine protease motif, sequences were identified through BLAST using EspL from EPEC E2348/69 as a reference. A section of the proteins identified by BLAST were aligned using Clustal Omega and presentation of alignment performed using ESPript3 [39]. Accession numbers (same order as displayed in Supplementary Figure Fig. 2) CAS10778, AIG70345, WP_012905388, WP_031942474, WP_024259347, ENZ84489, WP_023263817, WP_015872003, WP_020957625, CCA83579, WP_009667375, CDG86051, WP_004389152, WP_004714204, WP_019080404, AHK18540, WP_002211641, AIN16488.

A set of protein sequences was curated based on the identification of homologues of EspL from EPEC E2348/69. BLAST [25] was used to compare these protein sequences to the *nr* database and *nt* database (downloaded on 31st July from ftp://ftp.ebi.edu.au/pub/databases/ncbi/blast/db/) with blastp and tblastn respectively to identify additional proteins. The subsequent results were filtered on the E scores of 0.0 and length, and reduced to unique accession (removing duplicates). The nucleotide sequences were translated into amino acid sequences with EMBOSS [40] and the protein sequences were aligned with Muscle [41]. The best fitting protein model was determined using the Perl script ProteinModelSelection.pl available at http://sco.hits.org/exelixis/web/software/raxml/ for RAxML [42]. One hundred

pseudo-replicate RAxML analyses were run three times using the best-fitting substitution model, PROTGAMMA VF. The best scoring Maximum Likelihood tree was selected and midpoint rooted in Dendroscope [43]. The following accession numbers were used for phylogenetic analyses; CAS10778.1, AIG70345.1, CBG87854.1, ACR69900, CP001064, CP011417, LM996972, LM997319, CP001064, Z54194, WP_ 028120439, LM996116, WP_028120664, WP_038348374, AJ303141 LM996576, AP010958, LM995478, LM995537, LM996653, LM997233, LM997407, LM995613, LM997087, WP_001121612, WP_001121619, WP_001121621, WP_033810450, WP_044863368, AAJV00000000, AIAN00000000, FM986650, AP010960, LM996367, EHW09036, EHW21689, WP_001121623, WP_001121627, WP_001121746, WP_001121747, WP_001121748, WP_021824236, WP_023981847, WP_032272532, WP_032273780, AIHA00000000, WP_032349748, AIHB00000000, AIHD00000000, AIHE00000000, AAJX00000000, AIBC00000000, LN554915, LM996042, LM996071, LM996922, WP_001121620, WP_032210130, AKNI01000047, AIAL00000000, AIAO00000000, AIGY00000000, AIGZ00000000, AIBX00000000, CP006262, CP007133, LM996313, LM996458, CP007136, LM995993, LM996803, LM997001, WP_001121622, AIAI00000000, AIAX00000000, AF453441, AIBD00000000, CP008805, CP001164, CP001368, CP001925, CP010304, EHV10408, WP_001121626, WP_024256897, WP_032208682, AIAQ00000000, LM995690, LM995751, LM995947, AJ277443, FM201463, LM995831, LM996694, LM997125, EHW62569, WP_001121617, WP_032345473, WP_045889142, AICF00000000, AIAC00000000, AIGK00000000, AIGN00000000, AIGO00000000, AIAG00000000, AIGL00000000, AIGM00000000, AIBT00000000, AIBR00000000, AIBV00000000, AIGX00000000, WP_001121628, CP001846, CP003109, WP_001121608, WP_001121609, WP_001121624, AIAH00000000, AIAD00000000, ADUL01000000, AIFD00000000, AIAE00000000, AIFS00000000, AIFT00000000, AIFU00000000, AIFQ00000000, FM986652, LM996749, CDG86051, WP_038497945, WP_009667375, CCA83579, FP885907, AEG72234, CBJ36034, CEJ16658, EUJ11993, WP_003265371, WP_003274329, WP_013209029, WP_039553678, WP_042549988, WP_042592182, WP_043947056, ENZ84489, CP000037, CP001062, WP_012421777, CP000035, CP006737, ADA76828, EFP73031, EFW48342, WP_000608472, WP_005015229, WP_011379052, AY879342, NG_035859, NG_035867, AF348706, AF386526, AL391753, AY879342, CP001384, CP007038, Z54211, CAA90938, EIQ30821, WP_005058548, WP_005061014, WP_005065444, WP_005115993, WP_005117432, WP_010921597, WP_010921642, WP_015060143, WP_024259347, WP_025746267, WP_025748914, WP_025759433, WP_025766126, WP_031942474, WP_039060413, WP_040234710, WP_047204882, WP_047204897, CP000039, CP011423, HE616529, WP_005041841, WP_005138925, WP_024261348, CFB70006, CFQ67145, CNC44257, CRE36360, WP_019080404, CFR06093, WP_004389152, CP000305, CP001585, CP001589, CP001608, CP002956, CP009492, CP009704, CP009723, CP009785, CP009836,CP009844, CP009973, CP009996, CP010023, CP010293, AE009952, AE017042, AL590842, CP000308, CP001593, CP009840, CP009906, CP009991, KGA51839, WP_002211641, WP_045123609, BX936398, CP001048, CP009757, CP009780, CP009786, CP010067, CP000950, CP008943, CP009712, CP009759, CP009792, CFV36814, CNG55237, CNJ16181, WP_011193035, WP_012104544,

WP_012303595, ESJ22116.1, WP_032466541, WP_038400874, WP_004714204, CP007230, CNC46702, WP_025381344, WP_006576111.1

Mouse infection studies

All animal experimentation was approved by the Melbourne University Animal Ethics Committee. All mice used were of a C57BL/6 background and were age matched as best as possible between 5-8 weeks pre-infection. No calculation was used to assess the number of animals required. Male and female mice were allocated to experimental groups to ensure even distribution of age, sex and weight and investigators were not blinded to the allocation. *Citrobacter rodentium* was cultured in LB broth overnight before centrifugation and re-suspension in PBS to a concentration of ~5 x 10^9 cells/mL. C57BL/6 (5- to 8 weeks old) were inoculated by oral gavage with 200 μl of approximately 1 x 10^9 c.f.u of *C. rodentium*. The viable count of the inoculum was determined retrospectively by plating dilutions of the inoculum on plates with appropriate antibiotics. Mice were weighed every 2 days and faeces collected every 2 or 4 days for enumeration of c.f.u. The viable count per g of faeces was determined by plating serial dilutions of faeces onto media containing selective antibiotics.

Statistical analysis

All statistical analyses were performed using GraphPad Prism version 6.0. Statistical tests used were unpaired two-tailed Student's *t*-test for pairwise comparisons between groups or One-way ANOVA with Holm-Sidak's Test for multiple comparisons where indicated. Variance was similar in all comparisons. Differences in faecal counts of CR from mice and diarrhoea and pathology scores were assessed using a Mann Whitney U test, where normal distribution was not assumed. $P < 0.05$ was considered to be significant.

Supplementary Material

Refer to Web version on PubMed Central for supplementary material.

Acknowledgments

We gratefully acknowledge Edward Mocarski (Emory University) for the gift of Flag-ZBP1/DAI and Flag-M45 and Gabrielle Belz (Walter and Eliza Hall Institute) for animal ethics assistance. We thank Sam Young (Walter and Eliza Hall Institute) for technical assistance. This work was supported by the Australian National Health and Medical Research Council (Program Grant ID606788 to ELH, Project Grants APP1057888 to JS and APP1051210 to JV and APP1057905 to JMM and JS; Fellowships APP1090108 to JSP, APP1052598 to JV and APP1105754 to JMM) and the Australian Research Council (Future Fellowship FT130100166 to UN, Discovery Project DP150104227 to MS). CG and DI were supported by Australian Postgraduate Awards. TW was supported by a University of Melbourne International Research Scholarship (MIRS). GNS is funded by the Medical Research Council, UK. This work was made possible through Victorian State Government Operational Infrastructure Support and Australian Government NHMRC IRIISS. The authors declare no financial interests related to this work.

Data availability

The data that support the findings of this study are available from the corresponding author upon request

References

1. Sun X, Yin J, Starovasnik MA, Fairbrother WJ, Dixit VM. Identification of a novel homotypic interaction motif required for the phosphorylation of receptor-interacting protein (RIP) by RIP3. J Biol Chem. 2002; 277: 9505–9511. [PubMed: 11734559]
2. Kaiser WJ, Offermann MK. Apoptosis induced by the toll-like receptor adaptor TRIF is dependent on its receptor interacting protein homotypic interaction motif. J Immunol. 2005; 174: 4942–4952. [PubMed: 15814722]
3. Rebsamen M, et al. DAI/ZBP1 recruits RIP1 and RIP3 through RIP homotypic interaction motifs to activate NF-kappaB. EMBO Rep. 2009; 10: 916–922. [PubMed: 19590578]
4. Li J, et al. The RIP1/RIP3 necrosome forms a functional amyloid signaling complex required for programmed necrosis. Cell. 2012; 150: 339–350. [PubMed: 22817896]
5. Pasparakis M, Vandenabeele P. Necroptosis and its role in inflammation. Nature. 2015; 517: 311–320. [PubMed: 25592536]
6. Micheau O, Tschopp J. Induction of TNF receptor I-mediated apoptosis via two sequential signaling complexes. Cell. 2003; 114: 181–190. [PubMed: 12887920]
7. Holler N, et al. Fas triggers an alternative, caspase-8-independent cell death pathway using the kinase RIP as effector molecule. Nat Immunol. 2000; 1: 489–495. [PubMed: 11101870]
8. Cho YS, et al. Phosphorylation-driven assembly of the RIP1-RIP3 complex regulates programmed necrosis and virus-induced inflammation. Cell. 2009; 137: 1112–1123. [PubMed: 19524513]
9. He S, et al. Receptor interacting protein kinase-3 determines cellular necrotic response to TNF-alpha. Cell. 2009; 137: 1100–1111. [PubMed: 19524512]
10. Murphy JM, et al. The pseudokinase MLKL mediates necroptosis via a molecular switch mechanism. Immunity. 2013; 39: 443–453. [PubMed: 24012422]
11. Sun L, et al. Mixed lineage kinase domain-like protein mediates necrosis signaling downstream of RIP3 kinase. Cell. 2012; 148: 213–227. [PubMed: 22265413]
12. Cai Z, et al. Plasma membrane translocation of trimerized MLKL protein is required for TNF-induced necroptosis. Nat Cell Biol. 2014; 16: 55–65. [PubMed: 24316671]
13. Hildebrand JM, et al. Activation of the pseudokinase MLKL unleashes the four-helix bundle domain to induce membrane localization and necroptotic cell death. Proc Natl Acad Sci USA. 2014; 111: 15072–15077. [PubMed: 25288762]
14. Kaiser WJ, et al. Toll-like receptor 3-mediated necrosis via TRIF, RIP3, and MLKL. J Biol Chem. 2013; 288: 31268–31279. [PubMed: 24019532]
15. Upton JW, Kaiser WJ, Mocarski ES. DAI/ZBP1/DLM-1 complexes with RIP3 to mediate virus-induced programmed necrosis that is targeted by murine cytomegalovirus vIRA. Cell Host Microbe. 2012; 11: 290–297. [PubMed: 22423968]
16. Lawlor KE, et al. RIPK3 promotes cell death and NLRP3 inflammasome activation in the absence of MLKL. Nat Commun. 2015; 6 6282 [PubMed: 25693118]
17. Giogha C, Lung TW, Pearson JS, Hartland EL. Inhibition of death receptor signaling by bacterial gut pathogens. Cytokine Growth Factor Rev. 2014; 25: 235–243. [PubMed: 24440054]
18. Pearson JS, et al. A type III effector antagonizes death receptor signalling during bacterial gut infection. Nature. 2013; 501: 247–251. [PubMed: 24025841]
19. Li S, et al. Pathogen blocks host death receptor signalling by arginine GlcNAcylation of death domains. Nature. 2013; 501: 242–246. [PubMed: 23955153]
20. Zhang L, et al. Cysteine methylation disrupts ubiquitin-chain sensing in NF-kappaB activation. Nature. 2012; 481: 204–208.
21. Charpentier X, Oswald E. Identification of the secretion and translocation domain of the enteropathogenic and enterohemorrhagic *Escherichia coli* effector Cif, using TEM-1 beta-lactamase as a new fluorescence-based reporter. J Bacteriol. 2004; 186: 5486–5495. [PubMed: 15292151]
22. Wertz IE, et al. De-ubiquitination and ubiquitin ligase domains of A20 downregulate NF-kappaB signalling. Nature. 2004; 430: 694–699. [PubMed: 15258597]

23. Newton K, et al. Ubiquitin chain editing revealed by polyubiquitin linkage-specific antibodies. Cell. 2008; 134: 668–678. [PubMed: 18724939]
24. Lin Y, Devin A, Rodriguez Y, Liu ZG. Cleavage of the death domain kinase RIP by caspase-8 prompts TNF-induced apoptosis. Genes Dev. 1999; 13: 2514–2526. [PubMed: 10521396]
25. Altschul SF, Gish W, Miller W, Myers EW, Lipman DJ. Basic local alignment search tool. J Mol Biol. 1990; 215: 403–410. [PubMed: 2231712]
26. Kelley LA, Sternberg MJ. Protein structure prediction on the Web: a case study using the Phyre server. Nat Protoc. 2009; 4: 363–371. [PubMed: 19247286]
27. Shao F, Merritt PM, Bao Z, Innes RW, Dixon JE. A *Yersinia* effector and a *Pseudomonas* avirulence protein define a family of cysteine proteases functioning in bacterial pathogenesis. Cell. 2002; 109: 575–588. [PubMed: 12062101]
28. Humphries F, Yang S, Wang B, Moynagh PN. RIP kinases: key decision makers in cell death and innate immunity. Cell Death Differ. 2015; 22: 225–236. [PubMed: 25146926]
29. Vince JE, et al. IAP antagonists target cIAP1 to induce TNFalpha-dependent apoptosis. Cell. 2007; 131: 682–693. [PubMed: 18022363]
30. Wickham ME, et al. Bacterial genetic determinants of non-O157 STEC outbreaks and hemolytic-uremic syndrome after infection. J Infect Dis. 2006; 194: 819–827. [PubMed: 16941350]
31. Conzen SD, Cole CN. The three transforming regions of SV40 T antigen are required for immortalization of primary mouse embryo fibroblasts. Oncogene. 1995; 11: 2295–2302. [PubMed: 8570180]
32. Hornung V, et al. Silica crystals and aluminum salts activate the NALP3 inflammasome through phagosomal destabilization. Nat Immunol. 2008; 9: 847–856. [PubMed: 18604214]
33. Tanzer MC, et al. Evolutionary divergence of the necroptosis effector MLKL. Cell Death Differ. 2016; 23: 1185–1197. [PubMed: 26868910]
34. Catanzariti AM, Soboleva TA, Jans DA, Board PG, Baker RT. An efficient system for high-level expression and easy purification of authentic recombinant proteins. Protein Sci. 2004; 13: 1331–1339. [PubMed: 15096636]
35. Galan JE, Ginocchio C, Costeas P. Molecular and functional characterization of the Salmonella invasion gene invA: homology of InvA to members of a new protein family. J Bacteriol. 1992; 174: 4338–4349. [PubMed: 1624429]
36. Datsenko KA, Wanner BL. One-step inactivation of chromosomal genes in *Escherichia coli* K-12 using PCR products. Proc Natl Acad Sci US A. 2000; 97: 6640–6645.
37. McKenzie GJ, Craig NL. Fast, easy and efficient: site-specific insertion of transgenes into enterobacterial chromosomes using Tn7 without need for selection of the insertion event. BMC Microbiol. 2006; 6: 39. [PubMed: 16646962]
38. Huang KF, Chiou SH, Ko TP, Yuann JM, Wang AH. The 1.35 A structure of cadmium-substituted TM-3, a snake-venom metalloproteinase from Taiwan habu: elucidation of a TNFalpha-converting enzyme-like active-site structure with a distorted octahedral geometry of cadmium. Acta Crystallogr D Biol Crystallogr. 2002; 58: 1118–1128. [PubMed: 12077431]
39. Gouet P, Courcelle E, Stuart DI, Metoz F. ESPript: analysis of multiple sequence alignments in PostScript. Bioinformatics. 1999; 15: 305–308. [PubMed: 10320398]
40. Coppolino MG, et al. Requirement for N-ethylmaleimide-sensitive factor activity at different stages of bacterial invasion and phagocytosis. J Biol Chem. 2001; 276: 4772–4780. [PubMed: 11092884]
41. Edgar RC. MUSCLE: a multiple sequence alignment method with reduced time and space complexity. BMC Bioinformatics. 2004; 5 113 [PubMed: 15318951]
42. Stamatakis A. RAxML version 8: a tool for phylogenetic analysis and post-analysis of large phylogenies. Bioinformatics. 2014; 30: 1312–1313. [PubMed: 24451623]
43. Huson DH, Scornavacca C. Dendroscope 3: an interactive tool for rooted phylogenetic trees and networks. Syst Biol. 2012; 61: 1061–1067. [PubMed: 22780991]
44. Levine MM, et al. Escherichia coli strains that cause diarrhoea but do not produce heat-labile or heat-stable enterotoxins and are non-invasive. Lancet. 1978; 1: 1119–1122. [PubMed: 77415]

45. Newton HJ, et al. The type III effectors NleE and NleB from enteropathogenic *E. coli* and OspZ from *Shigella* block nuclear translocation of NF-kappaB p65. PLoS Pathog. 2010; 6 e1000898 [PubMed: 20485572]

46. Garmendia J, et al. TccP is an enterohaemorrhagic *Escherichia coli* O157:H7 type III effector protein that couples Tir to the actin-cytoskeleton. Cell Microbiol. 2004; 6: 1167–1183. [PubMed: 15527496]

47. Mundy R, et al. Identification of a novel type IV pilus gene cluster required for gastrointestinal colonization of *Citrobacter rodentium* . Mol Microbiol. 2003; 48: 795–809. [PubMed: 12694622]

48. Kelly M, et al. Essential role of the type III secretion system effector NleB in colonization of mice by *Citrobacter rodentium* . Infect Immun. 2006; 74: 2328–2337. [PubMed: 16552063]

49. Yamamoto M, et al. A cluster of interferon-gamma-inducible p65 GTPases plays a critical role in host defense against *Toxoplasma gondii* . Immunity. 2012; 37: 302–313. [PubMed: 22795875]

Europe PMC Funders Author Manuscripts

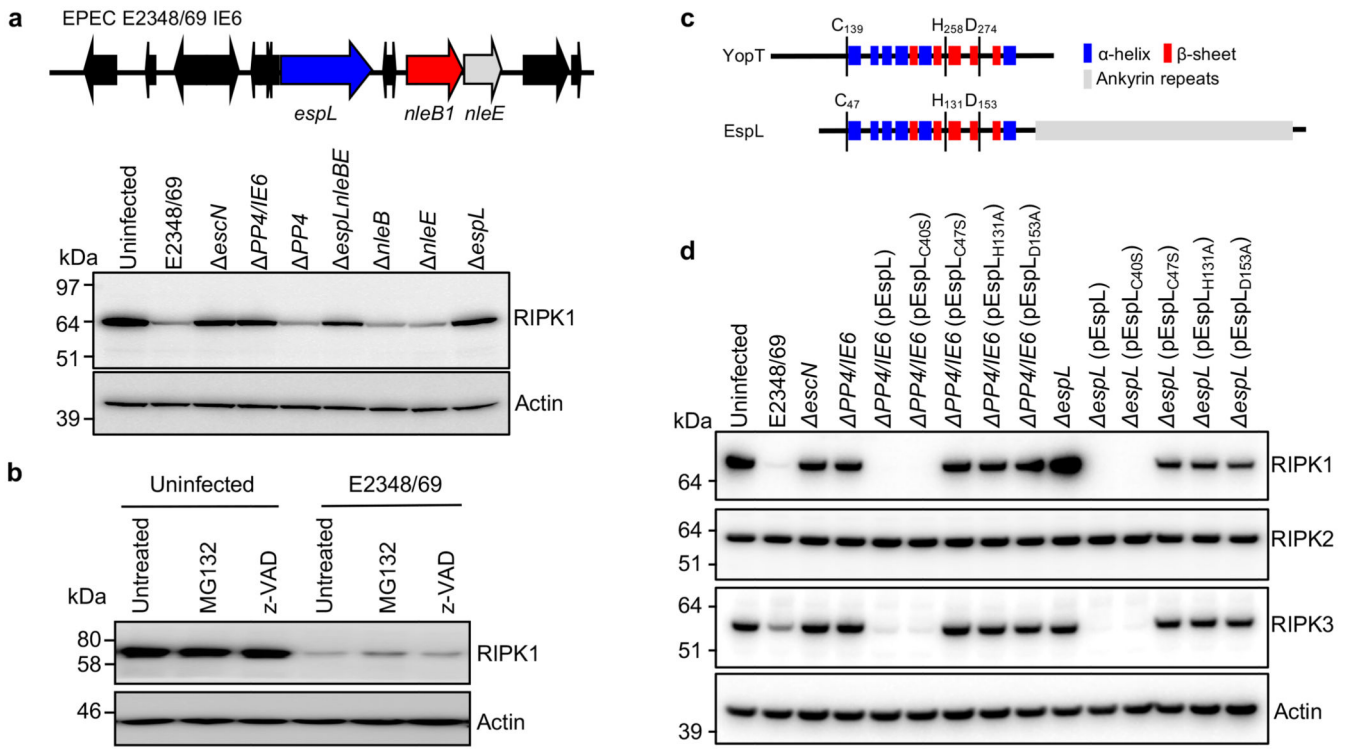

Figure 1. EspL is a T3SS cysteine protease that degrades RIPK1 and RIPK3.

a, Schematic representation of EPEC E2348/69 genomic integrative element 6 (IE6) harbouring *espL, nleB1*, and *nleE* and immunoblot showing RIPK1 degradation in HT-29 cells infected with derivatives of EPEC E2348/69 as shown. Representative immunoblot from at least 3 independent experiments. Actin; loading control. **b,** Immunoblot showing RIPK1 degradation in HeLa cells uninfected or infected with EPEC E2348/69; untreated, or treated with either MG132 or z-VAD-FMK (z-VAD). Representative immunoblot from at least three independent experiments. Actin; loading control. **c,** Schematic representation of cysteine protease motif and secondary structure predicted by Phyre in YopT from *Y. pestis* KIM and EspL from EPEC E2348/69. **d,** Immunoblot showing levels of RIPK1, RIPK2 and RIPK3 in HT-29 cells infected with derivatives of EPEC E2348/69. Representative immunoblot from at least three independent experiments. Actin; loading control.

Europe PMC Funders Author Manuscripts

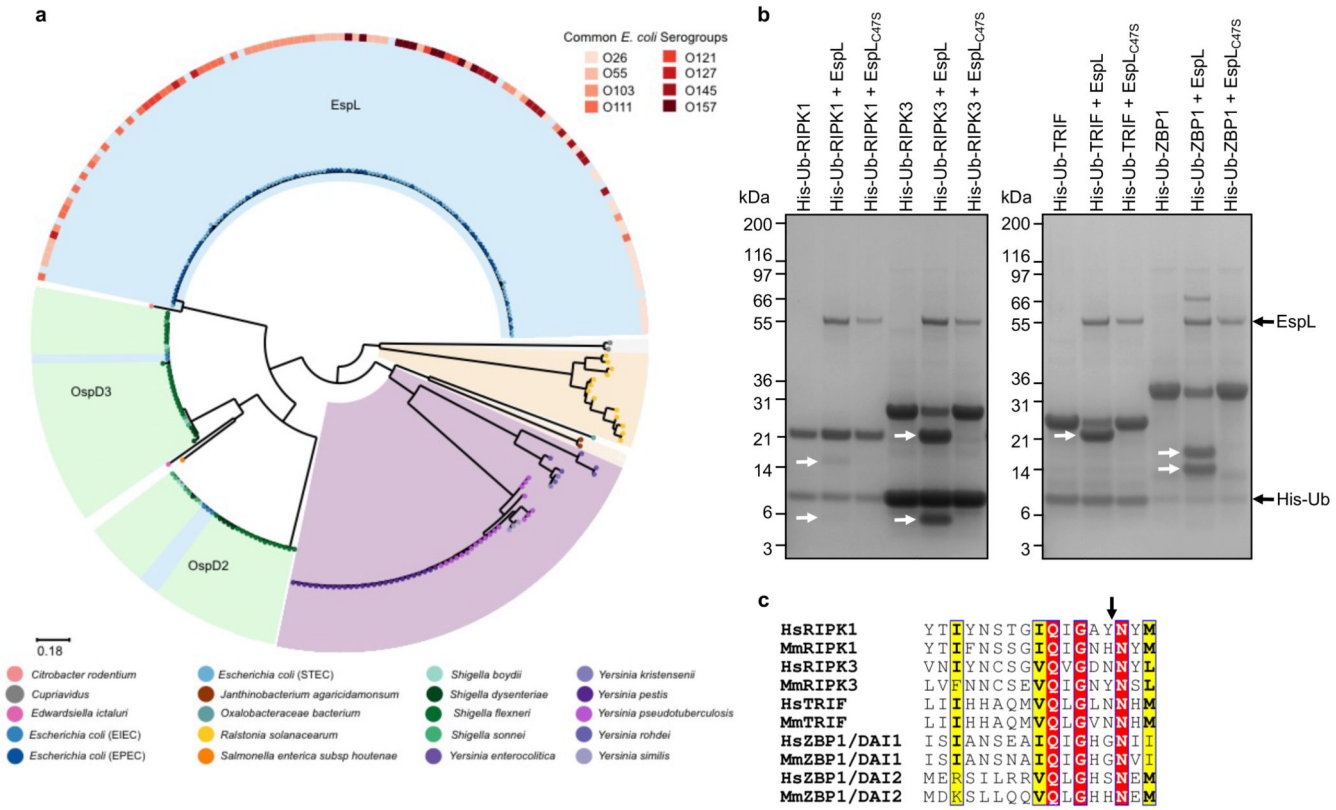

Figure 2. Distribution of EspL in Gram negative pathogens and substrate specificity.

a, Phylogeny of EspL homologues from a range of Gram negative pathogens which was midpoint rooted. Different genera are highlighted by background colour and the tips are coloured by species or pathotype. **b,** Coomassie Brilliant Blue stain of SDS PAGE gel showing *in vitro* cleavage of purified RHIM-containing regions of RIPK1, RIPK3, TRIF and ZBP1 (expressed as recombinant His6-ubiquitin-tagged proteins) by purified recombinant EspL. Representative gel from at least two independent experiments. Purified recombinant $EspL_{C47S}$ was used as a negative control. White arrows indicate cleavage products. Black arrows indicate EspL and the band corresponding to free His_6-ubiquitin (His-Ub) Note, observed cleavage product derived from ZBP1/DAI was consistent with EspL cleavage in first RHIM of ZBP1/DAI. **c**, EspL cleavage site indicated by an arrow in the RHIM containing regions of RIPK1, RIPK3, TRIF and ZBP1/DAI. Alignment was performed using Clustal Omega and ESPript3. Cleavage sites in RIPK3 and TRIF were determined experimentally by mass spectrometry and N-terminal sequencing.

Europe PMC Funders Author Manuscripts

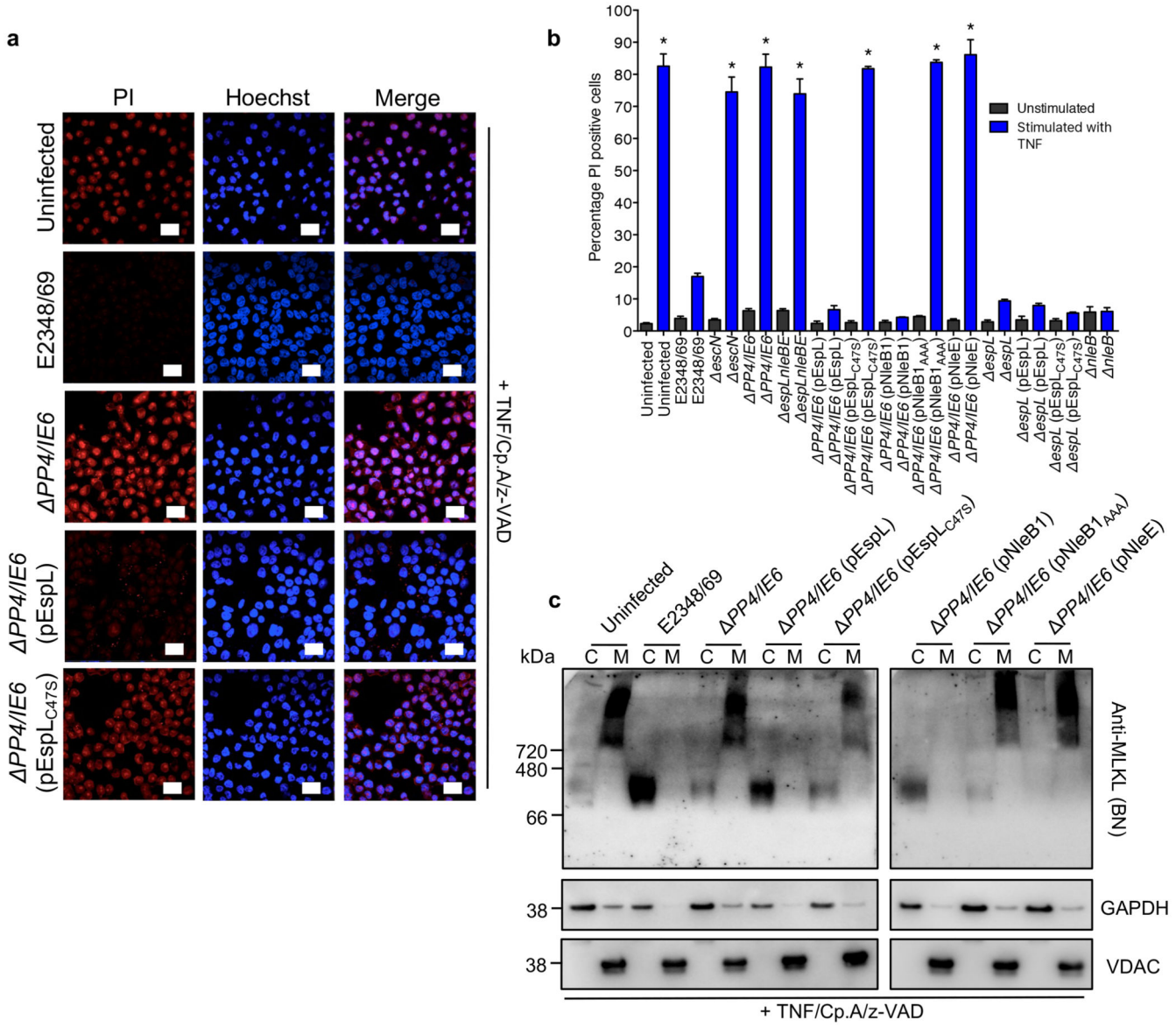

Figure 3. EspL inhibits TNF-induced necroptosis.

a, Cell death visualised by propidium iodide (PI) staining in HT-29 cells infected with derivatives of EPEC and treated with TNF, compound A (Cp.A) and z-VAD-FMK (z-VAD). Hoechst; stain for nucleic acid. Scale bar, 20 μm. Representative images shown from at least three independent experiments. **b,** Quantification of PI staining from microscopic analysis in HT-29 cells infected with derivatives of EPEC E2348/69 and treated with TNF, Cp.A and z-VAD. Results are mean ± s.e.m. percentage of cells positive for PI staining from three independent experiments counting ~200 cells in triplicate. *P<0.0001 compared to EPEC E2348/69 infected cells, one-way ANOVA with Holm-Sidak multiple comparison. **c,** Blue native PAGE analysis of MLKL membrane translocation in HT-29 cells infected with derivatives of EPEC E2348/69 treated with TNF, Cp.A and z-VAD. Representative immunoblot from at least three independent experiments. GAPDH; cytosolic fraction loading control, VDAC; membrane fraction loading control.

Europe PMC Funders Author Manuscripts

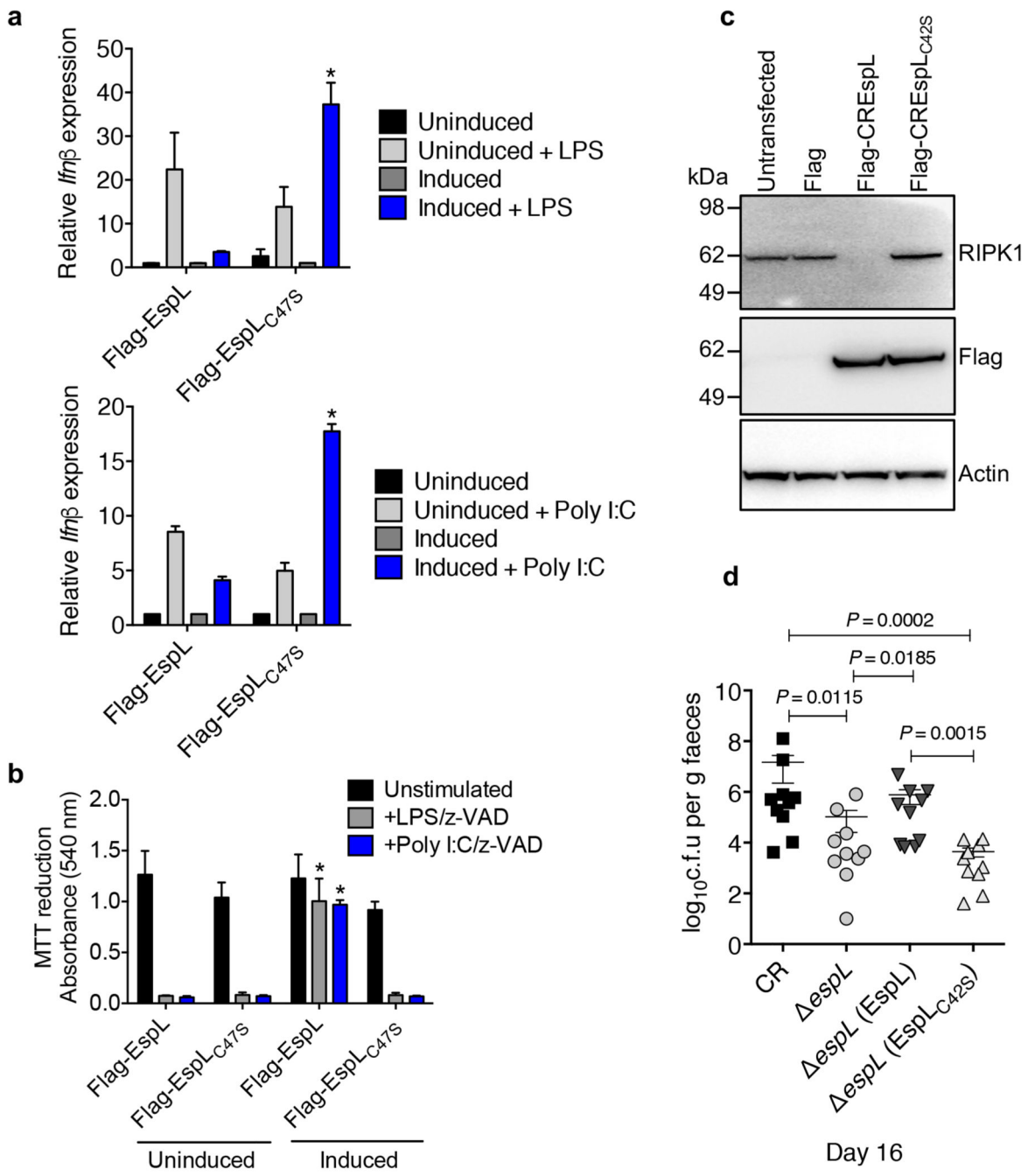

Figure 4. EspL activity inhibits TLR3/4-mediated signalling and contributes to *in vivo* persistence.

a, *Ifnβ* expression in doxycycline-inducible iBMDMs stably expressing either Flag-EspL or Flag-EspL$_{C47S}$ and treated with either LPS or Poly I:C for 3 h as indicated. Results are mean ± s.e.m of at least three independent experiments performed in triplicate. *Ifnβ* expression relative to uninduced, unstimulated cells. *P<0.0005 compared to Flag-EspL induced with doxycycline and treated with LPS or poly I:C, unpaired, two-tailed *t*-test. **b,** MTT reduction in doxycycline-inducible iBMDMs stably expressing either Flag-EspL or Flag-EspL$_{C47S}$

and treated with either LPS/z-VAD or Poly I:C/z-VAD for 20 h. Results are mean ± s.e.m. of absorbance at 540 nm from three independent experiments performed in triplicate. *P< 0.05 compared to Flag-EspL_{C47S} induced with doxycycline and treated with LPS or poly I:C, unpaired, two-tailed t-test. **c,** Immunoblot showing degradation of endogenous RIPK1 by EspL from *C. rodentium* (Flag-CREspL) but not EspL_{C42S} (Flag-CREspLC42S) expressed ectopically in HEK293T cells. Representative immunoblot from at least three independent experiments. **d,** Bacterial load in the faeces of mice 16 days after infection with derivatives of *C. rodentium*, including wild type *C. rodentium* ICC169 (CR), an *espL* deletion mutant *(ΔespL)* and *ΔespL* complemented with *espL* (EspL) or *espL*$_{C42s}$ (EspL_{C42S}) by Tn *7* transposition. Each data point represents $\log_{10}$ c.f.u. per g faeces per individual animal (c.f.u., colony forming units). Mean ± s.e.m. are indicated. Data was combined from three independent experiments. *P* values from Mann–Whitney U-test.

Europe PMC Funders Author Manuscripts